

Biogenic synthesis and characterization of gold nanoparticles using *Vitis vinifera* seed extract: Exploring antioxidant, anti-inflammatory and anti-cancer activities

Kowsalya B¹, Narendhirakannan RT^{1*}, Sinouassane D², Mariya AAV¹ & Venkatesh R¹

¹Department of Biochemistry, Kongunadu Arts & Science College (Autonomous), G.N. Mills P.O., Coimbatore-641 029, Tamil Nadu, India

²Department of Biomedical Science, Universiti Tunku Abdul Rahman (UTTAR), Kampar, Perak-31900, Malaysia

Received 20 April 2025; revised 27 July 2025

The synthesis of gold nanoparticles (AuNPs) using a newly developed green approach shows great potential because of its non-toxic and eco-friendly properties. In this study, biosynthesis of AuNPs was prepared using aqueous seed extract of *Vitis vinifera*. The presence of AuNPs was confirmed by UV-Vis spectroscopy, which revealed a peak at 550 nm, A Fourier-transform infrared (FTIR) study shows spectra that are identical to functional groups and X-ray diffraction (XRD) analysis demonstrated that AuNPs were of excellent purity with crystalline cubic structure phases in nature. Scanning electron microscopy (SEM) demonstrated the objects usual spherical shape and smooth surface, while Transmission electron microscopy (TEM) investigation demonstrated a spherical morphology with particle sizes ranging from 5 nm to more. Energy dispersive x-ray spectroscopy (EDX) confirmed the presence of Au elements at 2.2 keV. Also, evaluated antioxidant activity observed more effective and suggesting that they may possibly reduce damage produced by oxidative stress. The anti-inflammatory activity had a stronger effect, indicating their potential use in the treatment of inflammatory diseases. Further, the results of *in vitro* cytotoxicity activity of the samples against (HT-29) cell lines demonstrated the highest percentage of cell cytotoxicity. Therefore, all of these findings show that AuNPs produced through the plant-mediated method of synthesis may be cost-effective and environmentally safe, and that they may have interesting biological activity that could lead to biomedical application.

Keywords: AuNps, Cytotoxicity, Nanoparticles, *Vitis vinifera*

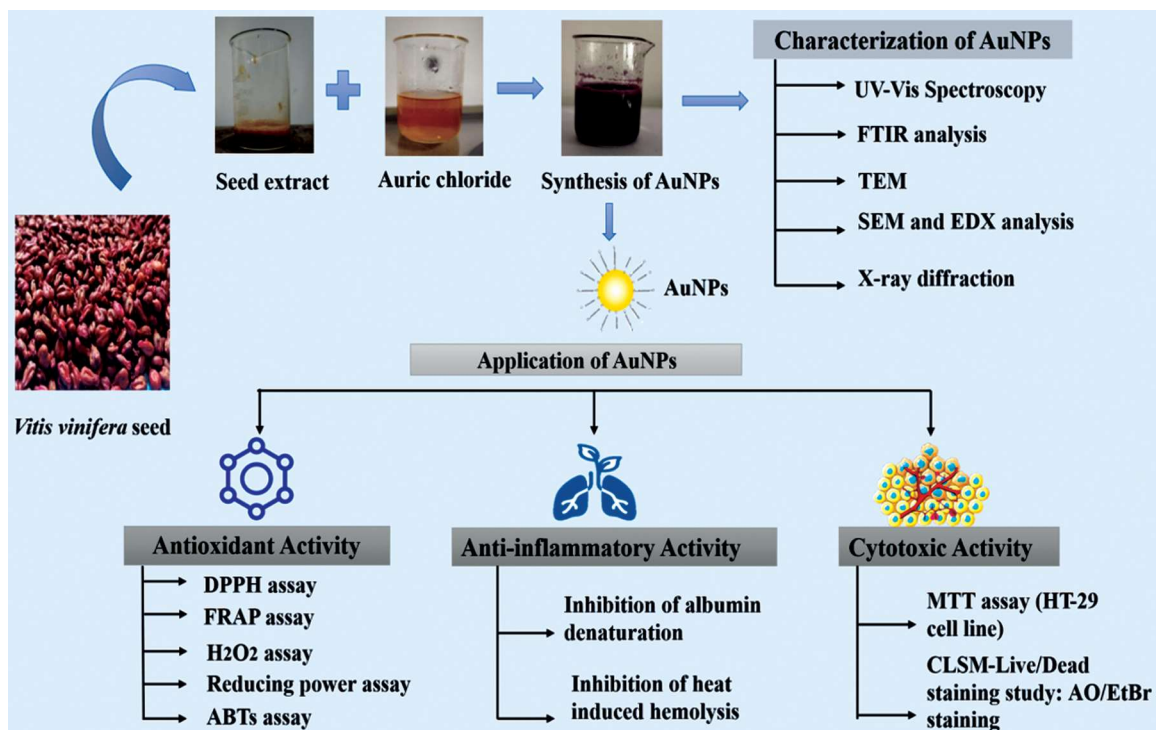
Nanotechnology, an important 21st century technology, is made up of atoms at the nanoscale, which can be as small as 1 nanometre or as large as 100 nm. Chemistry, Physics, and Medicine are just a few of the disciplines where it has impacted research¹. Nanoparticles have a wide range of applications in Chemistry, water treatment, cancer treatment, drug delivery, food safety, textiles, and photocatalysis, in addition to their cytotoxic, antibacterial, and antioxidant qualities, researchers have become very interested in synthesising nanoparticles from metals. Additionally, nanoparticles increase pharmaceuticals stability and solubility, increasing the efficacy of medications with low water solubility. They are useful in precision medicine and combination therapy techniques because of their versatility, which enables concurrent administration of therapeutic medications, targeting ligands, and imaging agents². Furthermore, nanoparticles are essential for diagnostic applications,

helping to assess the effectiveness of therapy and enable early cancer diagnosis³.

Metal nanoparticles made of noble metals, such as gold (Au), are among the most significant kinds. As versatile agents with a wide range of applications, gold nanoparticles (AuNPs) have made significant advances in biology and medicine. Gold and other metallic nanoparticles are frequently employed as nanomaterials for theranostic cancer treatment applications. It is utilised in the biomedical field for very sensitive biomolecular screening, cellular therapeutic delivery, protein tagging, selective cell annihilation of cancer cells by photothermal therapy, and other particular cells. It is because they offer a variety of imaging and diagnostic techniques, gold nanoparticles have emerged as crucial tools in the fight against cancer⁴. Gold nanoparticles have a wide range of applications in modern biology and medicine research. Clinical chemistry, biosensors, genomics, immunological analysis, optical bioimaging, targeted drug delivery, the identification and photothermalization of bacteria and cancer cells, antigens, and DNA, and

*Correspondence:

E-mail: rtnaren@kongunaducollege.ac.in



Graphical abstract

the tracking of cells and tissues with modern registration systems are all included in this. In recent years, the most promising applications of gold nanoparticles in biological and medical research have surfaced. Numerous biological effects, including antibacterial, anti-inflammatory, antioxidant, cytotoxic, antidiabetic, anticancer, and photocatalytic qualities, have been documented for gold nanoparticles made from various plant components. Recent research has examined the synthesis of AuNPs using plants like *Azadirachta indica*⁵, and the green biosynthesis approach (AuNPs) has been reported to be a promising option for producing AuNPs. The possibility of gold NP as therapeutic agents for conditions like cancer has been investigated.

Cancer has become the greatest critical problem and the major reason for death in the world. It is major global public health issue, even with rapid developments in diagnosis and treatment⁶. According to⁷, colorectal cancer is a diverse disease that progresses to the formation of polyps, which are malignant tumours in the inner walls of the colon and rectum. The WHO reports (2018) referred to colorectal cancer as the second most common cause of death globally and the third most common cancer, according to the International Agency for Research on Cancer (IARC). However, colon cancer can be

benign, non-cancerous, or malignant, depending on the severity of the condition. Significant developments in nanomedicine have given rise to cancer detection and treatment. Due to low toxicity of AuNPs compared to other metal nanoparticles, it showed a predominant preference in medical applications, especially due to low toxicity. Gold nanoparticles also shown outstanding diagnostic and therapeutic uses, including biosensors, targeted distribution of anticancer medications, and enzyme-linked immunosorbent assays. Furthermore, because of their reducing capacity, natural extracts can stabilise nanoparticles made from them, increasing their cytotoxicity to tumour cells while causing minimal harm to non-tumor cells, making them an excellent substitute for conventional medications⁸. In the past, gold nanoparticles that can accurately encapsulate these molecules using a few processes and green synthesis have been presented. Moreover, as they particularly encapsulate bioactive chemicals with the highest cytotoxic activity, many of these nanoparticles can have a stronger therapeutic effect than the extract from which they are generated⁹.

Numerous ethnopharmacological investigations have demonstrated the advantageous application of plant-mediated medications in the treatment of various conditions, as plant-based medications are

recognised to be safe, trustworthy, and reasonably priced. Additionally, because plants contain advantageous biomolecules like alkaloids, flavonoids, phenolic glucosides, and protein that reduce metal ions to nanoparticles, the field of plant-based mediated nanoparticle research has grown in recent years¹⁰. These plant phytochemical elements play a significant role, which has led to the search for new, low-toxicity anti-inflammatory, antioxidant, and anticancer medications.

A popular fruit with several health benefits and a high nutritious content is Grapes, scientifically called as *V. vinifera*, belongs to Vitaceae family, grows throughout the Mediterranean and Central Asia, grapes are the most important fruit crop in the world. With an annual production of over 75 million tonnes worldwide. From this perspective, grapes and their products such as wine, grape juice, and preserves, are economically significant and have a big impact on waste production. There is a risk of contamination since residues such as marc, grape peels, and seeds remain because of poor management procedures. On the other hand, grape waste material is a rich source of vital nutrients, including vitamins, minerals, fats, proteins, carbs, and polyphenols¹¹. However, it is well known that the winemaking industry produces large amounts of byproducts, and disposing of them offers both financial and environmental difficulties. Food waste has raised serious concerns about public health. Therefore, researches to address global nutritional inadequacies and to turn food waste into a useful resource is worthwhile. Grape seed extract, a byproduct of wine production and a source of proanthocyanidins, has shown promise in a number of experimental studies. Its pharmacological action and positive health effects have been validated by studies showing its efficacy against diabetes, cancer, cardiovascular disease, inflammation, peptic ulcers, microbiological infections, and hypertension. Given their many uses, grape seed extracts have the potential to become a promising treatment¹². Grape seed extract has shown protective effects in animal studies, such as reducing the size of myocardial infarcts and inhibiting lipid peroxidation and DNA disruption. *In vitro*, it has been demonstrated to suppress human cancer cell lineages. To the best of our knowledge, this is the first study to report on the cytotoxicity, anti-inflammatory, and antioxidant properties of AuNPs made from *V. vinifera* aqueous seed extract. The study involves synthesising AuNPs from seed aqueous extracts of *V. vinifera* species. Following that, the produced

AuNPs were detailed characterization, and their biological activities were examined.

Materials and Methods

Sample collection

V. vinifera from the Coimbatore district of Tamil Nadu, India, was used in this study. In the wine industry, grape seeds were gathered from the Kalapatti region in Coimbatore. Sterile deionized water was used after tap water to wash the gathered seed. The seeds were ground into a fine, gritty powder after being shade-dried. The resulting powder was kept in storage for further research.

Extraction

10 grams of powder were added to a 100 mL of distilled water to create an aqueous extract, which was then extracted for 4 h in a heating mantle at 35°C. For future research, the resulting aqueous extract was condensed and stored.

Bio reduction of gold nanoparticles

20 mL of auric chloride solution (1 mM) were combined with the 10 mL aqueous extract of *V. vinifera* seeds. For 10 min, the reaction mixtures were incubated at 40–60°C. The reaction mixture had turned dark violet after around 10 min. The creation of gold nanoparticles (AuNPs) is visually confirmed by this colour shift¹³. The violet-coloured solution that was produced was saved for later characterization studies.

Characterization of nanoparticles

UV-vis spectra analysis

Using UV-vis-NIR, Jasco, V-670, the UV spectrum of biosynthesized AuNPs from *V. vinifera* seed was captured in order to investigate the bio-reduction activity. Test samples were subjected to spectral analysis using wavelengths ranging from 380 to 800 nm.

FTIR analysis

Fourier-transform infrared (FTIR) spectroscopy (SHIMADZU, IRSpirit) was used to analyze the biosynthesized AuNPs from *V. vinifera* seed in order to confirm the presence of functional groups. At a resolution of 16 cm⁻¹, the transmittance spectra were captured in the wave number range of 4000 to 600 cm⁻¹.

Scanning electron microscope (SEM) analysis

The resultant biosynthesized AuNPs from *V. vinifera* seed were examined for size and surface shape using a scanning electron microscope. A ZEISS EVO device was used to record the SEM results.

Energy-Dispersive X-ray analysis

The EDS X-ray spectrophotometer, which is typically combined with the current SEM (ZEISS EVO equipment), was used to perform the EDX analysis of biosynthesized AuNPs from *V. vinifera* seed.

Transmission electron microscope (TEM) analysis

The size, location, and shape of the biosynthesized AuNPs from *V. vinifera* seed were investigated using TEM. Carbon pre-coated copper grids (200 Kv) obtained from Bharathiar University in Coimbatore were used in this experiment. On the grid surface, a single drop of the sample solution which consisted of water and dispersed nanoparticles was left to air dry at 25°C. Using electron microscopes, the dried grids were examined at the required magnification (JEOL JEM 2100 TEM).

X-ray diffraction studies

The biosynthesized AuNPs from *V. vinifera* seed were subjected to X-ray diffraction investigations. The Rigaku Miniflex 600 X-ray diffractometer was used to characterize the objects in the current study. The X-ray source was Cu K radiation (1.5406), which produced diffraction patterns in the 10-80° range at room temperature (25°C) with a step value of 0.02°.

The Debye-Scherrer equation, which reads $D = k\lambda/\beta\cos\theta$, was used to calculate the average size. where D is the nanocrystals thickness, k is a constant, λ is the X-ray wavelength, and β is the breadth at half maximum at Bragg's angle 2θ .

Antioxidant activity**DPPH radical scavenging assay**

The method was modified by¹⁴ was used to test each extract's capacity to scavenge DPPH radicals. When DPPH radicals are reduced by an antioxidant substance, their greatest absorption occurs at 515 nm. 100 μ L of AuNPs from *V. vinifera* seed extract was combined with 3 mL of the DPPH• solution in aqueous (6×10^{-5} M), which was made every day. After 20 min of incubation at 37°C in a water bath, the samples absorbance at 515 nm decreased, and this was quantified (AE). Every day, a blank sample was made using 100 μ L of methanol in DPPH solution, and its absorbance (AB) was measured. Experiments were performed in triplicate. Radical scavenging activity was calculated using the following formula:

$$\% \text{ inhibition} = [(AB - AE)/AB] \times 100 \quad \dots (1)$$

where AB = absorbance of the blank sample, and AE = absorbance of the AuNPs from *V. vinifera* seed extract.

ABTS assay

The ABTS radical cation decolourisation experiment¹⁵, which is predicated on the reduction of ABTS+• radicals by antioxidants of the AuNPs from *V. vinifera* seed extract tested, was also used to investigate the free radical scavenging ability of plant extracts. Deionised water was used to dissolve ABTS to a concentration of 7 mM. The ABTS solution was reacted with 2.45 mM potassium persulfate (final concentration) to create the ABTS radical cation (ABTS+•). The mixture was then let to stand in the dark at 20°C for 12 to 16 h prior to use. In order to achieve an absorbance of 0.7 (± 0.02) at 734 nm, the ABTS+• solution was diluted in either ethanol or deionised water for the investigation. A suitable solvent blank reading (AB) was obtained. 10 min after the initial mixing (AE), the absorbance reading was taken at 30°C after 100 μ L AuNPs from *V. vinifera* seed extract solutions were added to 3 mL of ABTS+• solution. Every determination was made in triplicate, and every solution was used on the day of preparation. The formula was used to determine the percentage of inhibition of ABTS+•.

$$\% \text{ inhibition} = [(AB - AE)/AB] \times 100 (1)$$

where AB = absorbance of the blank sample, and AE = absorbance of the AuNPs from *V. vinifera* seed extract.

Ferric reducing antioxidant power assay

A modified FRAP assay was used to measure the ferric reducing capacity of AuNPs from *V. vinifera* seed extract¹⁶. This technique relies on the reduction of a colourless ferric complex (Fe³⁺-tripiryridyltriazine) to a blue ferrous complex (Fe²⁺-tripiryridyltriazine) at low pH due to the action of antioxidants that donate electrons. The change in absorbance at 593 nm is used to track the decline. Every day, 10 volumes of 300 mM acetate buffer (pH 3.6), 1 volume of 10 mM TPTZ (2,4,6-tri(2-pyridyl)-s-triazine) in 40 mM hydrochloric acid, and 1 volume of 20 mM ferric chloride were combined to create the functional FRAP reagent. A standard curve was created utilising different FeSO₄ × 7H₂O concentrations. The day of preparation involved the usage of every solution. 3mL of freshly made FRAP reagent were mixed with one hundred microlitres of

sample solutions and three hundred microlitres of deionised water. In a water bath, the reaction mixture was incubated for 30 min at 37°C. The samples absorbance was then measured at 593 nm. Additionally, a sample blank reading was obtained using acetate buffer. The FRAP value was determined by calculating the difference between sample absorbance and blank absorbance. The reducing capacity of the plant extracts under test was determined in this assay using the reaction signal provided by a Fe²⁺ solution. mmol Fe²⁺/g of material was the unit of measurement for FRAP results. All measurements were done in triplicate.

Reducing power assay

AuNPs from *V. vinifera* seed extract was tested for reducing power using the methodology of¹⁷. Potassium ferricyanide (1.0 mL, 10 mg/mL), phosphate buffer (1 mL, 0.2 M, pH 6.6), and AuNPs from *V. vinifera* seed extract (0.1 mL, 1.0 mg/mL). Extract (1 mg/mL), potassium ferricyanide (1.0 mL, 10 mg/mL), and phosphate buffer (1 mL, 0.2 M, pH 6.6) were combined and incubated for 20 min at 50°C. After adding 100 mg/ml of trichloroacetic acid (1.0 mL), the mixture was centrifuged for five min at 13,400 ×g. After adding ferric chloride (0.1 mL, 1.0 mg/mL) and distilled water (1.0 mL) to the supernatant (1.0 mL), the absorbance was measured at 700 nm.

H₂O₂ radical scavenging assay

A hydrogen peroxide solution (2 mM/L) was made using standard phosphate buffer (pH 7.4). AuNPs from *V. vinifera* seed extract at various concentrations in distilled water were combined with 0.6 millilitres of hydrogen peroxide solution. A blank solution containing phosphate buffer but no hydrogen peroxide was used to assess absorbance at 230 nm after ten min. The percentage inhibition of the extracts at different dosages was compared using the ascorbic acid standard. In all of the above techniques, the percentage inhibition was calculated using the formula¹⁸.

$$\% \text{ Radical scavenging} = (\text{Control OD} - \text{Test OD}) / \text{Control OD} \times 100$$

Anti-inflammatory activity

Inhibition of albumin denaturation assay

The methods described in¹⁹ were used to perform the experiment. adding a few modifications, such limiting each reaction mix component's volume in half. The AuNPs from *V. vinifera* seed extract and positive standards, ibuprofen and diclofenac, were

made at a concentration of 0.1% (1.0 mg/mL) each. Each combination was prepared in a reaction jar with 200 µL of egg albumin, 1400 µL of phosphate buffered saline, and 1000 µL of the test extract. Instead of extracts, distilled water was used as a negative control. Following a 15 min incubation period at 37°C, the mixtures were heated to 70°C for five min. After cooling, a Spectrophotometer was used to measure the absorbances at 660 nm, and the data was analysed by the Spectra Manager system. The following formula was used to determine the inhibition % of protein denaturation.

$$\% \text{ Denaturation inhibition} = (1 - D/C) \times 100\%$$

Where D is the absorbance reading of the test sample, and C is the absorbance reading without test sample (negative control).

Heat induced hemolysis assay

The control tubes were only used with saline solution. 2 mL of the reaction mixture consist of 1mL of 10% RBC solution and 1mL of AuNPs from *V. vinifera* seed extract in varying quantities. Each tube was cooled to 56°C for 30 min using tap water. Following a five-minute, 2500 rpm centrifugation of the test tubes, the absorbance of the supernatant was measured at 560 nm²⁰. Three runs of the experiment were performed for every test specimen. The inhibitory percentage or acceleration of hemolysis specific to each test was calculated using the following formula.

$$\% \text{ inhibition of hemolysis} = 100 - [1 - (\text{OD2} - \text{OD1} / \text{OD3} - \text{OD1})]$$

Where OD1 equals the test sample unheated, OD2 equals the test sample heated and treated, OD3 equals control heated sample.

Anti-cancer activity

MTT assay

The MTT assay was used to evaluate AuNPs from *V. vinifera* seed extract cytotoxic effect on HT-29 cells. The lactate dehydrogenase enzyme, which is produced by mitochondria, transforms MTT, a tetrazolium salt, into insoluble purple formazan crystals²¹. The cells were plated in a 96-well plate at a density of 15,000 and incubated at 37°C for the entire night. This was done in 200 µL of appropriate medium. Following cell adhesion to the cell culture plate surface, DMEM containing different working concentrations of the test chemical (12.5, 25, 50, 100,

and 200 µg/mL) was added to replace the spent media. After a drug was added, the cells were incubated for 24 h at 37°C in an atmosphere with 5% CO₂. Following incubation, 100 µL of MTT (0.5 mg/mL) was added to the cells, and they were incubated for 3hrs at 37°C. The formazan crystals were dissolved in 100µL of DMSO, and a microplate reader (ELX-800, BioTek, USA) was used to measure the purple colour at 570 nm. Cells fed with DMEM alone were thought to be 100% viable. The following formula is used to determine the percentage of cell viability:

$$\% \text{ cell viability} = [\text{OD of treated cells} / \text{OD of Untreated cells}] \times 100$$

The IC₅₀ value was determined by using linear regression equation i.e. $Y = Mx + C$. Here, $Y = 50$, M and C values were derived from the viability graph.

Cell morphological assessment

After being treated with the specified test substances for 24 h at 37°C at doses ranging from 12.5 µg/mL to 200 µg/mL, the morphological alterations in HT-29 cells were evaluated. With the use of a camera and MICAM software, cells were viewed and captured at a 20x magnification using an Inverted Biological Microscope (CKX-41, Olympus). 100 µM is the scale.

Dual staining (AO/EtBr) study by confocal live cell imaging system

Green fluorescence is produced when the Acridine Orange (AO) dye conjugates with every cell. Cells without cytoplasmic membranes will react with Ethidium Bromide (EtBr) staining; when DNA is interpolated, the nucleus will appear red. Benchtop fluorescence microscopy shows that cells going through early apoptosis exhibit high green fluorescence, whereas live cells have green nuclei. Green patches represent condensed chromatin, whereas reddish-orange cells are thought to be late apoptotic cells²². With minor adjustments to the earlier work and based on prior experience. Incubate cells in a 6-well plate at a density of 0.5×10^6 cells/2 mL for 24 h at 37°C in a CO₂ incubator. Aspirate the spent medium and wash with 1mL of 1x PBS. In 1 mL of culture media, treat the cells with the appropriate concentration of the test chemical (AuNPs from *V. vinifera* seed extract) and controls, then incubate them for a full day. The untreated/control group consisted of cells that received no treatment. After the treatment is complete, empty the medium from each well into a 5 mL tube and rinse with 500 microlitres of PBS (don't

forget to keep the PBS in the same tubes). To separate the cells from the plate surface, remove the PBS and add 500 µL of trypsin-EDTA solution. Then, incubate for 3-4 min at 37°C. Harvest the cells straight into 5 mL tubes after returning the culture media to their individual wells. The tubes should be centrifuged at $300 \times g$ for five min at 25°C. Decant the supernatant carefully. Rinse twice with PBS. Drain the PBS thoroughly. For 10 min, stain cells with 200 µL of staining solution (AO+EtBr dye mixture). After 5 min of centrifuging the tubes at 1000 rpm, remove the staining solution and rinse with PBS to get rid of any leftover dye. Fill each well of a 35mm glass bottom dish with 100ul of cell culture, then use a filter cube and a fluorescence microscope to see the results. For EtBr, use excitation 560/40 nm and emission 645/75 nm, and for Acridine orange, use excitation 470/40 and emission 525/50 nm. Image J Software v1.48 was used to overlay the images.

Results

Bio-reduction of gold nanoparticles

In this study, gold nanoparticles were effectively synthesized in a very short amount of time using the seed extract from *V. vinifera*. The seed extract was initially pale-yellow in colour, then it changed to vibrant violet, indicating the synthesis of AuNPs (Fig. 1). Larger particle sizes are typically indicated by a dark violet colour in AuNPs solutions. Because of variations in their surface plasmon resonance (SPR), larger AuNPs tend to appear violet, whereas smaller ones are usually red. Larger particles tend to absorb shorter wavelengths and reflect longer ones, which causes a purple colour shift. This is because they absorb and scatter light differently. Thus, the reduction of Au³⁺ ions to Au nanoparticles can be facilitated by *V. vinifera* seed extract acting as an electron shuttle.

Characterization of nanoparticles

UV Vis Spectra analysis

UV-Vis spectroscopy is more commonly used and often considered a standard technique, especially for plasmonic nanoparticles like gold nanoparticles

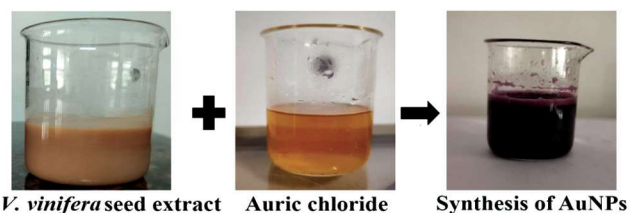


Fig. 1 — Synthesis of AuNPs from *V. vinifera* seed extract

(AuNPs). The analysis of UV-Vis spectra for AuNPs synthesized with *V.vinifera* seed revealed clear absorption peaks indicating the formation of nanoparticles. AuNPs synthesized with *V. vinifera* seed extract exhibited a prominent peak at approximately 550 nm (Fig. 2), indicative of the presence of gold nanoparticles displaying characteristic surface plasmon resonance (SPR) absorption. These spectroscopic features demonstrate the successful synthesis of gold nanoparticles utilizing *V. vinifera* seed extract as environmentally friendly reducing and stabilizing agents

FTIR analysis

FTIR spectra are used to determine which potential biomolecules are in charge of the reduction of Au³⁺ ions and the capping of the reduced AuNPs that are produced using seed extract from *V. vinifera* (Fig. 3). 3718.76, 1743.65, 1527.62, 1396.46, 1026.13, 686.66, 601.79, 563.21, 532.35, 501.49, and 462.92 were the areas with the strongest infrared bands. The spectrum

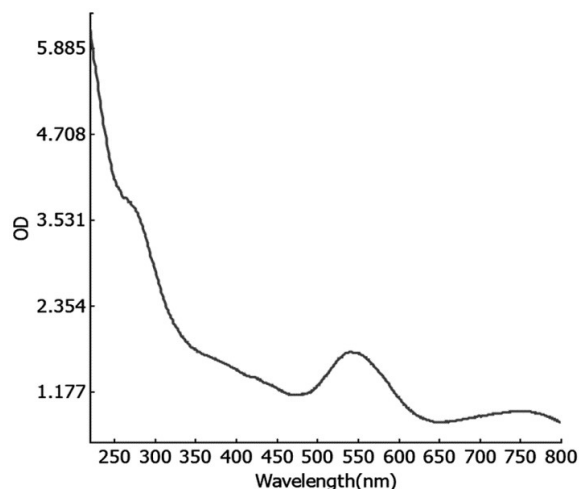


Fig. 2 — UV spectra of *V. vinifera* seed mediated AuNPs

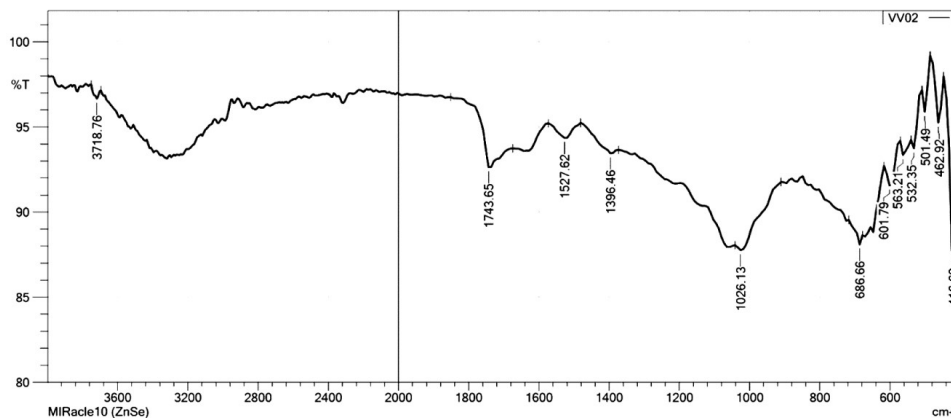


Fig. 3 — FTIR spectrum of *V. vinifera* seed mediated AuNPs

peaks of frequency, bond, and functional groups are displayed in (Table 1). In the FTIR spectrum of seed extract, the synthesis of AuNPs may be the cause of the tiny deviation in the IR absorption peaks.

Scanning Electron Microscope (SEM) analysis

While SEM is excellent for morphological characterization of nanoparticles, according to the SEM image, AuNPs made at room temperature (25°C) are spherical and rod-shaped, with an average size of 10 to 500 nm (Fig. 4). *V. vinifera* seed mediated AuNPs were widely distributed and substantially agglomerated.

Energy-dispersive x-ray analysis

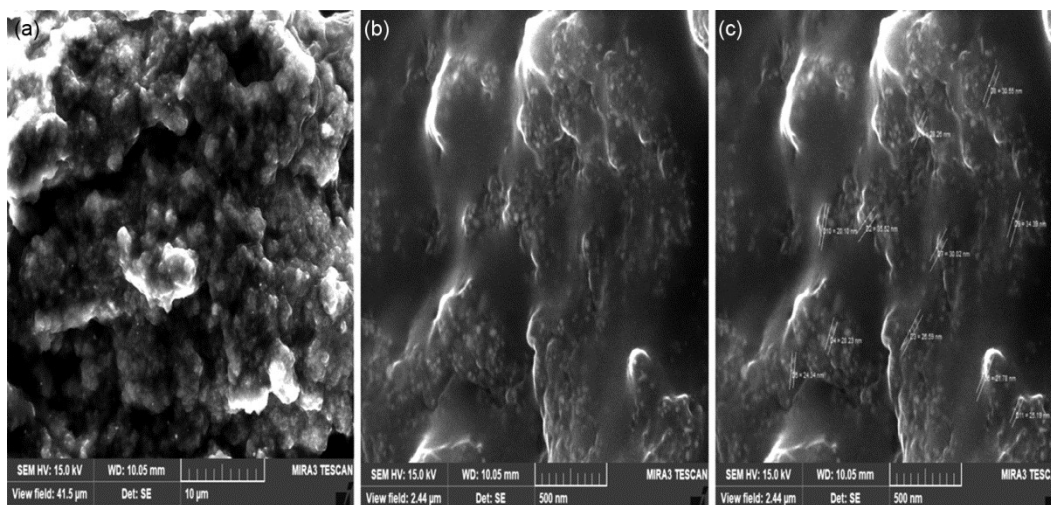
Energy Dispersive X-ray Spectroscopy (EDX) was utilized to collect information on the chemical composition of materials for elements with atomic numbers (Z) greater than 3. The produced AuNPs spectra showed distinctive absorption peaks when analysed using EDX. Interestingly, each AuNPs spectrum showed a noticeable absorption peak at 2.2 keV, which is characteristic of absorption of gold (Fig. 5). This peak verifies that gold is present in the produced nanoparticles since it matches the distinctive X-ray emission line of gold (Au).

Transmission electron microscopy (TEM) analysis

While TEM is excellent for morphological characterization of nanoparticles, it is also a valuable tool for determining particle size and size distribution. TEM's high resolution allows for direct imaging of individual nanoparticles, revealing their shape, size, and how they are arranged. It can also be used to assess particle dispersion and identify any agglomeration. The produced AuNPs unique shapes were visible in TEM pictures. It is noteworthy that most of the nanoparticles had hexagonal, spherical and triangular shapes (Fig. 6), suggesting that the

Table 1 — FT-IR spectroscopic analysis of *V. vinifera* seed mediated AuNPs showing IR range and functional group

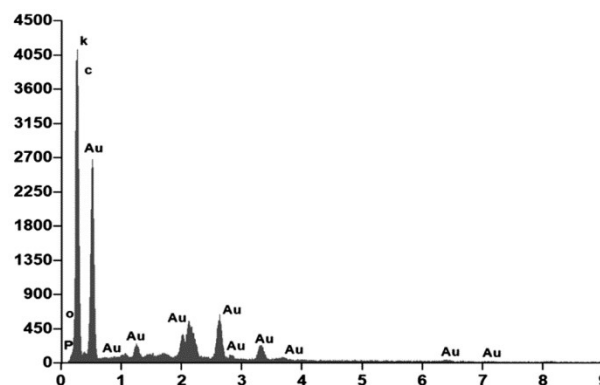
S. No	Frequency (cm ⁻¹)	Bond	Functional groups
1	3718.76	O-H stretch	Phenols
2	1743.65	C=O stretch	Aldehyde
3	1527.62	N-O stretch	Nitro compound
4	1396.46	C-F stretch	Fluro compound
5	1026.13	C=O stretch	Hydroxyl group
6	686.66	=C-H bending	Halo compound
7	601.79	C-Cl bending	Halo compound
8	563.21	C-H bending	Carbohydrates
9	532.35	C-Br stretch	Alkyl halides
10	501.49	C-Cl stretch	Halo compound
11	462.92	C-I stretch	Halo compound

Fig. 4 — SEM analysis of *V. vinifera* seed mediated AuNPs. (a) View in 10 μ m; (b) Overall view in 100 nm; and (c) Overall view in 100 nm with arrow marked

V. vinifera seed extracts had an impact on the shape-controlled synthesis of AuNPs. The TEM image indicates that the produced nanoparticles have a high degree of homogeneity and crystallinity. The *V. vinifera* seed mediated AuNPs were found to be between 20 and 100 nm in size on average.

X-ray diffraction studies

The crystalline quality of the nanoparticles was demonstrated by the clear peaks in the XRD pattern of the AuNPs that were generated using *V. vinifera* seed (Fig. 7). The (111), (200), (220), and (311) crystallographic planes of gold are represented by the conspicuous peaks seen at 2θ angles of 38.58° , 44.06° , 65.07° , and 78.23° , respectively. The face-centered cubic (fcc) gold structure is characterized by these peaks, which validate the synthesized AuNPs crystallinity. The purity of the produced nanoparticles is further supported by the XRD pattern's lack of impurity peaks. The *V. vinifera* seed mediated AuNPs are

Fig. 5 — EDX analysis of *V. vinifera* seed mediated AuNPs

crystalline indicates that the green synthesis method is successful in creating distinct crystalline nanoparticles.

Antioxidant activity

DPPH radical scavenging assay

The most well-known *in vitro* antioxidant test, the DPPH test, is easy to use, quick, dependable,

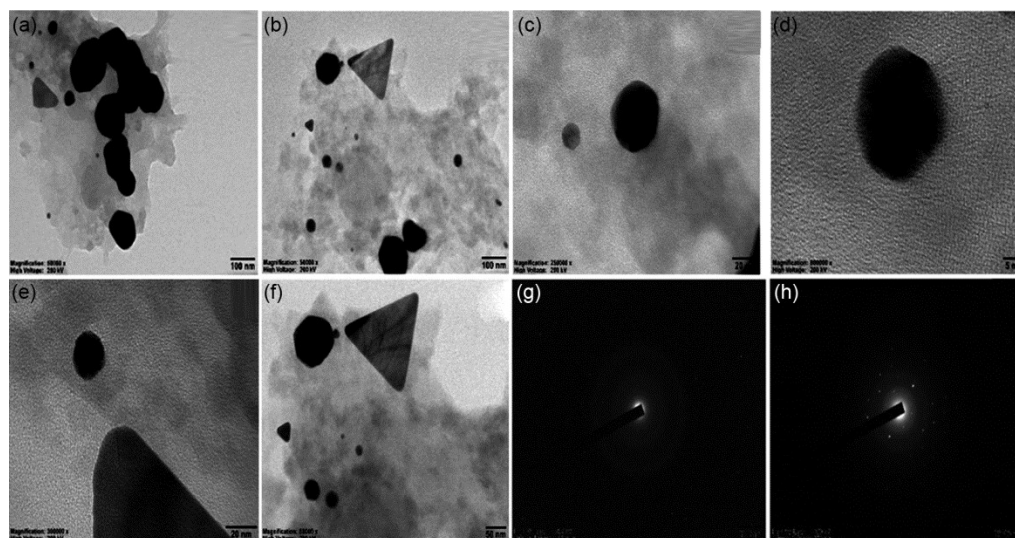


Fig. 6 — TEM analysis of *V. vinifera* seed-mediated AuNPs. (a & b) Overall view of sample; (c & d) TEM image illustrating thickness difference between hexagonal and spherical AuNPs; (e) HR-TEM image focused on angle feature of AuNPs; (f) HR-TEM image of individual triangular AuNPs; (g) SAED pattern of citrate gold nanoparticles; and (h) SAED pattern of 2DG Capped gold nanoparticles

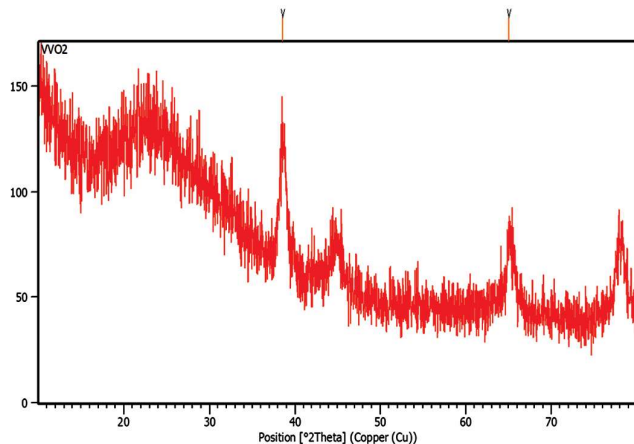


Fig. 7 — XRD analysis of *V. vinifera* seed mediated AuNPs

repeatable, and typically used to evaluate a compound's antioxidant capacity or efficacy. The biosynthesised AuNPs inhibited the DPPH radical in a concentration-dependent manner (Fig. 8a). The AuNPs mediated by *V. vinifera* seeds have demonstrated comparable DPPH scavenging activity. The AuNPs mediated by *V. vinifera* seeds have an IC_{50} value of 96.48 $\mu\text{g/mL}$.

ABTS assay

The ABTS assay, which gauges an antioxidant capacity to scavenge and prevent the generation of the ABTS radical cation, was used to assess the antioxidant activity of the seed-mediated AuNPs. Higher antioxidant activity was indicated by the percentage of inhibition rising as the concentration of the biosynthesised nanoparticles increased, as seen in

(Fig. 8b). AuNPs mediated by *V. vinifera* seed have an IC_{50} value of 103.24 $\mu\text{g/mL}$.

Ferric reducing antioxidant power assay

The ferric-reducing antioxidant capacity of the seed-mediated AuNPs was found to be more significant by the FRAP assay. (Fig. 8c) shows that the greatest FRAP value of seed-mediated AuNPs was recorded at an IC_{50} of 54.79 $\mu\text{g/mL}$.

Reducing power assay

By measuring the ability of antioxidants to supply electrons and repair oxidised molecules, the reducing power assay was used to evaluate the antioxidant activity of the biosynthesised AuNPs. Data of the seed-mediated AuNPs growing reduction power with increasing nanoparticle concentration is displayed in (Fig. 8d). *V. vinifera* seed-mediated AuNPs have an IC_{50} of 69.27 $\mu\text{g/mL}$.

H₂O₂ radical scavenging assay

The hydrogen peroxide radicals were efficiently quenched by the seed-mediated AuNPs. The biosynthesised AuNPs exhibited concentration-related hydrogen peroxide radical scavenging capability, as seen in (Fig. 8e). AuNPs mediated by *V. vinifera* seed have an IC_{50} of 85.25 $\mu\text{g/mL}$.

Anti-inflammatory activity

Inhibition of albumin denaturation assay

The inhibition of albumin denaturation assay, which measures the biosynthesised AuNPs' capacity to stop albumin denaturation, a protein marker for

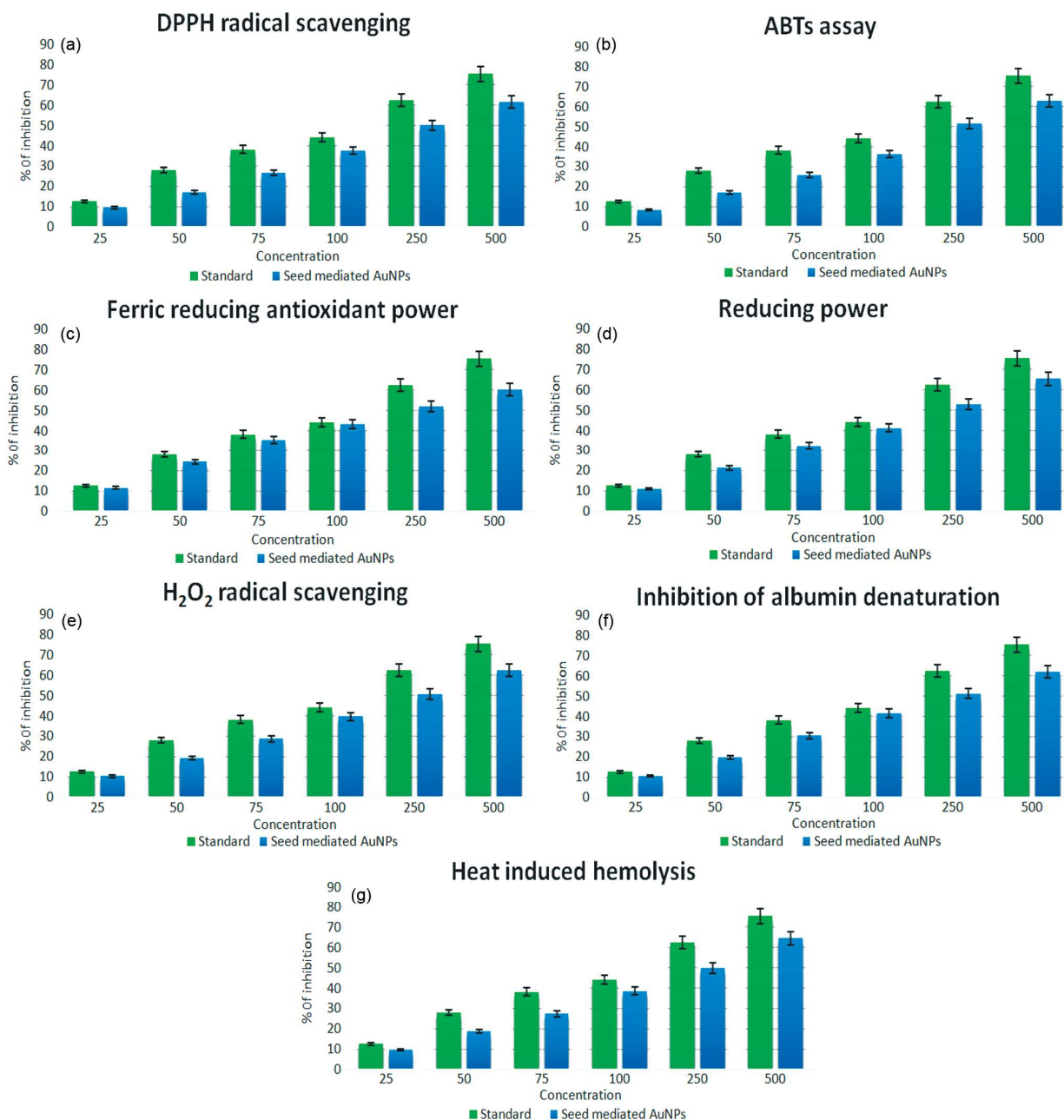


Fig. 8 — (a) DPPH radical scavenging activity; (b) ABTs activity; (c) FRAP activity; (d) Reducing power activity; (e) H₂O₂ radical scavenging activity; (f) Inhibition of albumin denaturation activity; and (g) Heat induced hemolysis activity of *V. vinifera* seed mediated AuNPs

inflammation, was used to assess the anti-inflammatory activity of the seed-mediated AuNPs. With IC₅₀ values of 76.60 µg/mL, (Fig. 8f) data showed that seed-mediated AuNPs showed the highest percentage inhibition of albumin denaturation. The anti-inflammatory activity of biosynthesized AuNPs was considerable, which displayed their potential to mitigate inflammation.

Heat induced hemolysis assay

By preventing red blood cell (RBC) membrane damage, a sign of inflammation, the heat-induced haemolysis assay was used to measure the anti-inflammatory effect of seed-mediated AuNPs. The biosynthesized AuNPs exhibited a dose-dependent response, meaning that haemolysis was more inhibited at higher doses (Fig. 8g).

V. vinifera seed-mediated AuNPs have an IC_{50} of 105.21 $\mu\text{g/mL}$.

Anti-cancer activity

MTT assay

The MTT assay, which measures cell viability and proliferation, is used to examine the anticancer activity of *V. vinifera* seed mediated AuNPs against the HT-29 cell line. Where cells are cultured on a plate and treated with varying concentrations of a test chemical to assess its effects. After adding the chemical, the cells are incubated for 24 h under controlled temperature and CO_2 conditions to ensure optimal growth and response. Under a phase contrast microscope, the morphological changes that followed incubation with seed mediated AuNPs at several concentrations were displayed, and the IC_{50} concentrations were also noted. The pictures are shown in (Fig. 9). The control groups cells showed no morphological changes, but the AuNPs treated group cells showed notable morphological alterations, including roundedness, a trait of stressed cells, irregular shape, cytoplasmic vacuolation, and growth.

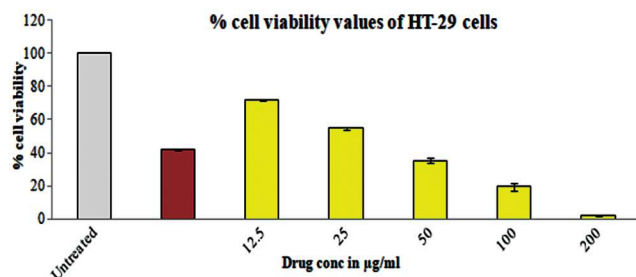


Fig. 9 — Overlaid bar graph depicted the % cell viability values of HT-29 cells treated with various concentrations of *V. vinifera* seed mediated AuNPs after the incubation period of 24 h

The biosynthesized AuNPs compare to conventional treatments, the study included 5-fluorouracil (5-FU), a widely used chemotherapeutic drug. At a 50 μM concentration, 5-FU resulted in 41.75% cell viability in the HT-29 cells. When compared to control groups, the anticancer action of AuNPs mediated by *V. vinifera* seeds showed a significant decrease in cell viability when compared to untreated cells (Table 2, and Fig. 10).

CLSM-Live/Dead staining study: AO/EtBr staining

Acridine orange (AO) and ethidium bromide (EB) dual staining were used in this study to analyse the CLSM-Live/Dead staining in HT-29 cells treated with gold nanoparticles (AuNPs) synthesised from *V. vinifera* seed (Fig. 11). The untreated cells, standard control cells, and *V. vinifera* seed mediated AuNPs treated with IC_{50} concentration represented changes in nuclear morphology of cells; AO stands for viable cells (green), and EtBr for dead cells (red). This variation in fluorescence intensity suggests that AuNPs elicit different apoptosis depending on where they are found in the *V. vinifera* seed (Fig. 12).

Table 2 — showed the % cell viability values of HT-29 cells and IC_{50} value of the *V. vinifera* seed mediated AuNPs against the Human colon cancer (HT-29) cells after the treatment period of 24 h

Condition	% cell viability \pm SD	IC_{50} conc ($\mu\text{g/mL}$)
Untreated	100	
5-fluorouracil-50 μM	41.75 \pm 0.13	29.44
12.5 μg	71.60 \pm 0.18	
25 μg	54.66 \pm 2.3	
50 μg	35.49 \pm 3.7	
100 μg	19.6 \pm 1.05	
200 μg	2.17 \pm 0.12	

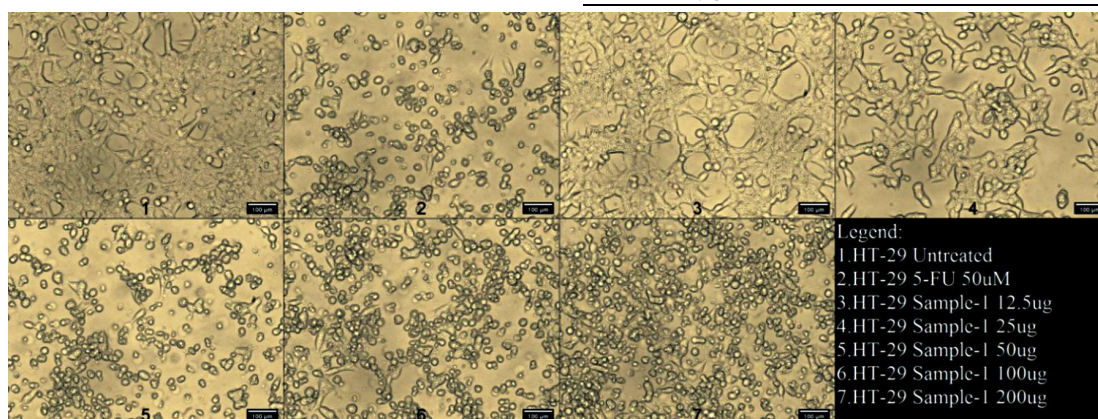


Fig. 10 — Overlaid montage photo represented the morphology of HT-29 cells treated by different concentrations of *V. vinifera* seed mediated AuNPs after the incubation period of 24h. All the images were acquired under the inverted biological microscope at 20x magnification and recorded with the help of Digital camera equipped with the MICAM software

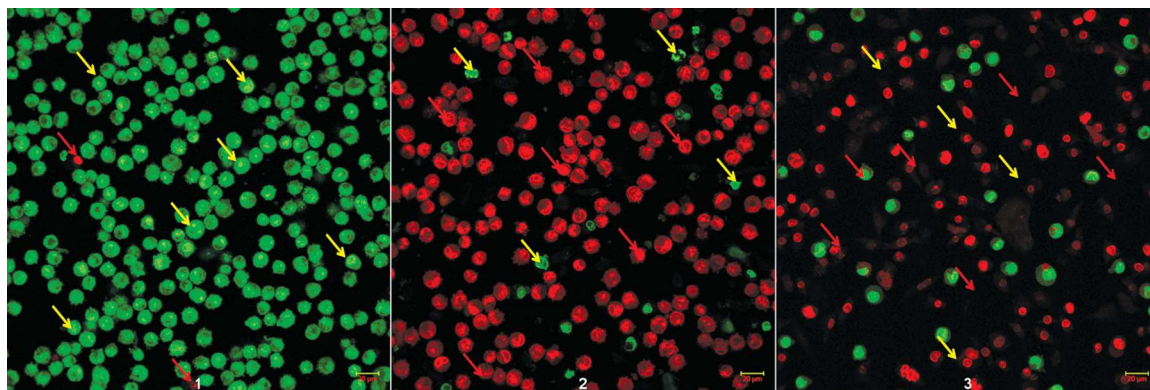


Fig. 11 — Acridine orange (AO) and Ethidium bromide (EB) dual staining study of HT-29 cells in Untreated, Std control and *V. vinifera* seed mediated AuNPs treated with IC_{50} concentration represented the changes in nuclear morphology of cells. AO represents viable cells (green colour) and EtBr represents dead cells (red colour). All the images were captured at 25x magnification. Legend: Yellow arrow-Viable/healthy cells and Red arrow-Dead or damaged cells

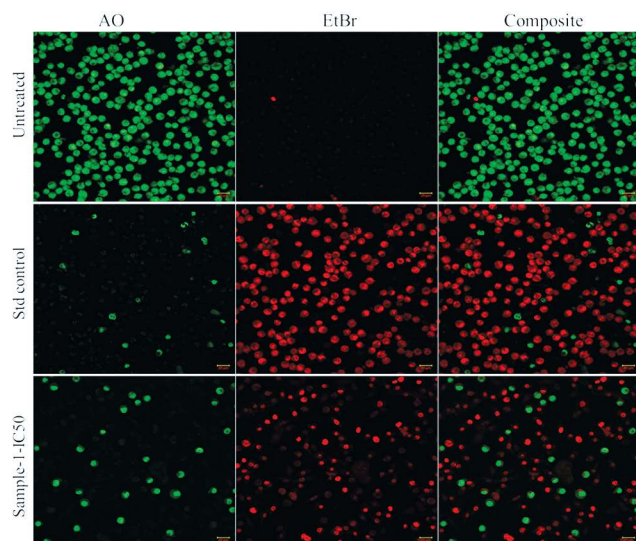


Fig. 12 — Composite overlaid image represented the Acridine orange (AO) and Ethidium bromide (EB) dual staining study of HT-29 cells in Untreated, Std control and *V. vinifera* seed mediated AuNPs treated with IC_{50} concentration represented the changes in nuclear morphology of cells. AO represents viable cells (green) and EtBr represents dead cells (red colour). All the images were captured at 25x magnification. Bright Green-stained nuclei indicates viable cells and Bright Red indicates-dead or damaged cells

Discussion

Metal nanoparticles made of noble metals, such as gold (Au), are among the most significant forms. Due to their multifunctional properties in therapeutics, detection, imaging, and surface modification, gold nanoparticles (NPs), which have been used in a wide range of applications in chemistry, material sciences, physics, medicine, and life sciences, must continue to grow exponentially. In addition to having a lower environmental impact, the synthesis of gold

nanoparticles using plant extract is beneficial since it can yield enormous amounts of nanoparticles. In the process of creating nanoparticles, plant extracts can function as stabilising and reducing agents.

The goal of this study is to examine the biological characteristics of AuNPs mediated by *V. vinifera* seeds and clarify how they might be used to fight cancer, inflammation, and oxidative stress. Nano-sized gold particles have been tested against a range of human cancer cells, and they are showing promise as cancer treatment agents. The chemical and other characteristics of gold nanoparticles are significantly influenced by their size and form. When compared to spherical nanoparticles, triangular-shaped nanoparticles exhibit appealing optical characteristics²³. Gold nanoparticles have transformed the medical field because of their numerous uses in targeted drug delivery, imaging, diagnosis, and therapeutics. These applications stem from their tenable optical, physical, and chemical properties, stability, non-cytotoxicity, and incredibly small size.

The solution turns from bright yellow to dark violet as a result of surface plasmon vibrations produced by biosynthesised gold nanoparticles. Visually, the colour of gold NP changed from colourless to light yellow and subsequently to dark violet when *V. vinifera* seed extract was added, as seen in (Fig. 1). The corresponding nanoparticles production is demonstrated by the colour variations that were seen during the experiment. Gold nanoparticles were detected by the colour changes in the solution, which were ascribed to the surface plasmon vibrations being activated. This could be due to the gold nanoparticles surface plasmon resonance (SPR) characteristics. UV-

vis spectroscopy has been analysed, the surface plasmon resonance for the production of AuNPs is responsible for the absorption peak at 550 nm in the UV-vis spectra (Fig. 2). According to²⁴, the SPR properties, which are reliant on the NPs' size, shape, and concentration, are what cause the colour variation in AuNP. The AuNPs-synthesised methanolic seed extract of *R. communis* displayed the gold absorbance peak at 550 nm, according to similar findings previously published by²⁵.

The FTIR analysis of the gold mediated nanoparticles *V. vinifera* seed extract is depicted in (Fig. 3). The gold showed minimum absorbance peak at 462.92 cm and 3718.76 cm in FTIR spectrum respectively. The gold NP showed 11 peak values (Table. 1). The extract's functional groups for the synthesized nanoparticles were identified using FTIR. Gold nanoparticles investigated showed the same functional groups phenols, aldehyde, nitro, halo and fluoro compounds, carbohydrates, and secondary alcohols. AuNPs demonstrated the existence of carboxylate and phenolic (alcoholic) functional groups, which are in charge of the binding with the AuNPs. According to²⁶, the carboxyl hydroxyl and aldehyde peaks in the FTIR spectra of CQDs containing *V. vinifera* seed extract were located at 4000 and 500 cm⁻¹, respectively.

SEM provides high-resolution images of individual nanoparticles, revealing their size, shape, and surface features. AuNPs from *V. vinifera* seed extract range in size from 25 to 50 nm, according to the SEM pictures (Fig. 4). Different-sized nanoparticles have a roughly spherical shape. Nonetheless, a few anisotropic nanostructures have also been observed, including nanorods, nanotriangles, and a few types of polygonal nano prisms. AuNPs made from *Sageretia thea* leaf extract had a spheroidal shape, but some of them changed to a rod-shaped form as the reaction medium became polydisperse. Prior research has documented the green manufacture of magnesium oxide nanoparticles with a spherical shape that are attached to *V. vinifera* extract²⁷.

Furthermore, the EDX investigation demonstrated that Au was present in the samples. Strong signals from the Au atom were detected in AuNPs at about 2.2 keV. Strong C and O signals were also present because of biomolecules that were exposed in (Fig 5) and involved in the AuNP cap of the *V. vinifera* seed. According to this study²⁸, the elements gold, carbon, and oxygen are clearly present in the AuNPs that are

formed from tangerine peel extract. A significant amount of gold in the composition is indicated by a strong peak at about 2.2 keV. The extract's constituents that are adsorbed onto the gold nanoparticles are responsible for the presence of carbon and oxygen.

TEM provides high-resolution, morphological images of the nanoparticle core, measuring the physical size of dried particles. The AuNPs with a range of morphologies, including hexagonal, spherical, and triangular shapes, and sizes between 20 and 100 nm have an average size, according to the transmission electron microscopy (TEM) images (Fig 6). Size measures the nanoparticle's physical dimensions, shape describes morphology spherical, rod-like, polyhedral, etc and location in TEM analysis of gold nanoparticles synthesized using seed extract refers to the spatial position of the particles within the sample. It includes whether they are evenly distributed or clustered on the TEM grid, and whether they're associated with or embedded in residual biomolecules derived from the extract. It also describes their relative proximity to each other highlighting if they exist as isolated particles or in aggregates and their presence within any remaining organic matrix, which indicates how seed derived biomolecules may be interacting with or stabilizing the nanoparticles. According to²⁹ the TEM result, the synthesis of gold nanoparticles mediated by *Mentha piperita* L. extract confirmed that the resulting morphological different shapes of nanohexagons and the smallest nanotriangles were different. This led to the conclusion that small nanotriangles can change over time into small nanohexagons, as shown by the semi-transformed triangle with an arrow. The *V. vinifera* seed AuNPs selected area electron diffraction (SAED) pattern (Fig. 6g and h) revealed the face-centered cubic (fcc) ring structure, which indicates the AuNPs higher degree of crystallinity. SAED patterns, which display spots from (111), (200), (220), and (311) Bragg's reflections of the FCC-Au lattice, verify that the crystal structures of the nanohexagons and nanotriangles are face-centered-cubic (FCC).

A popular and accurate method for determining the chemical structures and degree of crystallinity of synthesised nanoparticles is X-ray diffraction (XRD). They verified the size of those *V. vinifera* seed AuNPs as seen in (Fig 7) using XRD patterns. The XRD peaks in this experiment are located at $2\theta^\circ = 38.58^\circ$,

44.06°, 65.07°, and 78.23°, in that order. Likewise, the XRD results of gold nanoparticles with the highest intensity peaks at two theta values (38, 44, 64, and 78) demonstrated the FCC structure of AuNPs synthesised using the extract of ginger, neem, apta, and umber plants, as well as the type of gold nanoparticles formed after reducing HAuCl₄ by biological extracts³⁰.

The ability of some substances to reduce or prevent the harmful effects of free radicals in the body is known as antioxidant activity. Numerous secondary metabolites found in medicinal plants have a range of therapeutic applications and are dependable antioxidant sources. The plant extracts containing potent phytoconstituents produce stable AuNPs without the use of dangerous reducing agents, which are then used for biological applications. Consuming grape-derived dietary flavonoids, such as grape seed powder and grape extract, has been shown to successfully control oxidative stress and stop oxidative damage³¹.

Antioxidants eliminate oxidative stress and free radicals, which prevents the formation of radicals. Antioxidants are considered to be pioneers in the treatment of over a hundred problems. In-depth research has been done to identify natural antioxidants because of the harm that synthetic antioxidants produce³². Because they stop oxidation, they are also useful in food preservation. To assess a compound's ability to quench radicals, DPPH, a persistent free radical, is frequently used. This method is based on using a hydrogen-donating antioxidant to reduce DPPH, which produces the non-radical DPPH³³. The AuNPs employing *Bauhinia purpurea* leaf extract demonstrated DPPH radical scavenging efficacy, per³⁴.

An indicator of the antioxidant efficacy of chain-breaking antioxidants is the ABTS radical, which is produced when ABTS is oxidised. The radical scavenging activity of ABTs utilising biosynthesised AuNPs made from aqueous leaf extract of *Ziziphus nummularia*. According to³⁵, AuNPs made using fruit extract from *Sumac* (*Rhus coriaria*) were tested for their ability to scavenge radicals. The antioxidant qualities of medicinal plants and other natural substances can be evaluated using the FRAP (Ferric Reducing Antioxidant Power) assay. This experiment assessed the AuNPs of *V. vinifera* seed ability to use the reagent 2, 4, 6-tripyridyl-s-triazine (TPTZ) in a redox process to change ferric to ferrous ions³⁶ assessed the AuNPs, FRAP antioxidant efficacy

utilising extract from *Gelidiella acerosa*. The antioxidant capacity of *Hippophae rhamnoides* leaf and berry extract was assessed by measuring FRAP in their synthesis.

Compounds with reducing power can donate electrons and lower the oxidised precursors of lipid peroxidation processes since they are linked to antioxidant activity. The reducing power activity of AuNPs synthesised utilising *Sargassum muticum*, a brown macroalga, was assessed by³⁷. The hydrogen peroxide scavenging ability of the AuNPs generated from *V. vinifera* seed was also assessed in this investigation. due to the fact that hydrogen peroxide can enter the body through the skin, eyes, or lungs. The body rapidly breaks down H₂O₂ into oxygen and water, producing hydroxyl radicals that can cause DNA damage and lipid peroxidation³⁸. AuNPs utilising *Commiphora wightii* leaf aqueous extract demonstrated H₂O₂ scavenging ability, per³⁹.

Albumin denaturation inhibition and heat-induced haemolysis are two common *in-vitro* anti-inflammatory assays used to evaluate the possible anti-inflammatory properties of medications, extracts, and formulations. According to these assays assess the test chemicals capacity for reducing two forms of inflammation, including cell membrane damage and protein denaturation. AuNPs mediated by aqueous extracts from *V. vinifera* seeds have been studied. Excellent anti-inflammatory results were obtained from the albumin denaturation test. The AuNPs mediated from *Mentha Officinalis* similarly prevented albumin denaturation in a concentration-related manner, per the findings of⁴⁰. Using *Nicotiana plumbaginifolia*, the heat-induced haemolysis assay evaluated the potential of gold nanoparticles to protect red blood cell membranes from heat-induced damage, simulating the oxidative stress and membrane instability observed in inflammatory situations⁴¹.

The cytotoxic effects of AuNPs synthesized using *V. vinifera* seed extract on HT-29 colon cancer cells, revealing promising anticancer potential. The AuNPs exhibited a clear dose-dependent cytotoxicity, meaning that higher concentrations of nanoparticles resulted in greater cancer cell death. After a 24 h exposure period, cell viability significantly declined with increasing AuNP concentrations, as indicated in (Table 2). At 12.5 µg/mL, cell viability remained relatively high at 71.60%, but this dropped sharply to 2.17% at 200 µg/mL, demonstrating a strong inhibitory effect on cell proliferation. This trend

indicates a substantial capacity of the biosynthesized AuNPs to suppress cancer cell growth effectively. Although the precise IC_{50} value the concentration needed to inhibit 50% of cell viability is not explicitly provided, the results suggest that it lies between 100 $\mu\text{g/mL}$ and 200 $\mu\text{g/mL}$ (Fig. 9). This implies that the nanoparticles possess potent anticancer properties within a moderately high concentration range. To assess the comparative effectiveness of these biosynthesized nanoparticles, the study also examined the effect of a standard chemotherapeutic agent, 5-fluorouracil (5-FU), on HT-29 cells. At a concentration of 50 μM , 5-FU reduced cell viability to 41.75%, a value notably higher than the viability observed at equivalent or even lower concentrations of AuNPs, especially above 100 $\mu\text{g/mL}$ (Fig. 10). The AuNPs synthesized using *V. vinifera* seed extract demonstrate significant anticancer potential through a clear dose-dependent inhibition of colon cancer cell proliferation, and their performance relative to 5-FU highlights their promise as a natural and effective nanomedicine approach in cancer therapy. In a similar study, the extract from grape seeds was evaluated against two aggressive anticancer cell lines: Capan-2 pancreatic adenocarcinoma and triple negative breast cancer cell line⁴². The anticancer activity of the seed extract is significantly stronger. In contrast to the cells treated with *V. vinifera* seed gold nanoparticles, the results of⁴³ showed that apoptotic cells were clearly visible among the cells treated with the seed gold nanoparticles. Additionally, morphological changes, including roundedness, irregular cell shapes, and stressed cells, were evident in nearly all of the fluorouracil drug-treated cells in the A431 skin cancer cell line.

The morphological changes in HT 29 cell lines with *V. vinifera* seed AuNPs were examined using AO/EtBr double staining. The untreated cells did not exhibit any discernible alteration, as seen in (Figs. 11 and 12). HT-29 cell lines treated with AuNPs seed had a significant reddish-pale colour as a result of apoptotic cell death, which led to a significantly condensed nuclear content. Additional cells in the early stages of apoptosis displayed bubbling and a change in form. Similarly⁴⁴, when A431 cells were treated with AO/EtBr, *Vitis vinifera* seed extract-treated cells had a large number of necrotic and late apoptotic cells⁴⁵ found that human breast cancer cell lines showed a high potential for GNPs to kill cells because of their capacity to pass through cell membranes and influence the level of mRNA expression.

Conclusion

The study demonstrated that gold nanoparticles (AuNPs) synthesized using *Vitis vinifera* (grape) seed extract exhibit significant antioxidant, anti-inflammatory, and anticancer properties. The polyphenolic compounds present in grape seeds enhance the nanoparticle's ability to scavenge free radicals, thereby reducing oxidative stress and protecting cells from damage. Additionally, these nanoparticles inhibit pro-inflammatory cytokines, showcasing their potential in managing inflammatory disorders. In anticancer applications, AuNPs derived from *V. vinifera* seeds have shown efficacy against the HT-29 colon cancer cell line. Mechanisms include induction of apoptosis, suppression of cell proliferation, and inhibition of cancer cell migration. Their ability to reduce cancer cell viability in a dose-dependent manner, along with their comparable performance to standard drugs like 5-FU, underscores their therapeutic relevance. Due to their biocompatibility, these nanoparticles offer a promising alternative to conventional chemotherapy, with the advantage of selectively targeting cancer cells. Further studies, including detailed mechanistic evaluations and in vivo experiments, are needed to confirm their efficacy and safety. Overall, gold nanoparticles made from *V. vinifera* seeds have a lot of therapeutic potential. However, the current findings of AuNPs *V. vinifera* seed against the HT-29 cell line lay a strong foundation for considering these biosynthesized AuNPs as a promising candidate for future anticancer therapies

Acknowledgement

The authors are grateful to the management as well as the faculty members in the Department of Biochemistry, Kongunadu Arts and Science college (Autonomous) G.N. Mills P.O, Coimbatore, Tamil Nadu-641029, India for providing the support to fulfil this work.

Conflict of interest

All authors declare no conflicts of interest.

References

- 1 Gupta PC, Sharma N, Mishra P, Rai S & Verma T, Role of gold nanoparticles for targeted drug delivery. In: Metal and Metal-Oxide Based Nanomaterials: *Synthesis, Agricultural, Biomedical and Environmental Interventions*, (2024) 243.
- 2 Surale-Patil SA, Thorat VM, Jadhav SA, Chavda AV & Shah AS, Novel drug delivery systems for targeting tumor microenvironment. *J Res Ther Drug Deliv*, 7 (2023) 1.

- 3 Baranwal J, Barse B, Di Petrillo A, Gatto G, Pilia L & Kumar A, Nanoparticles in cancer diagnosis and treatment. *Materials*, 16 (2023) 15.
- 4 Oliveira BB, Ferreira D, Fernandes AR & Baptista PV, Engineering gold nanoparticles for molecular diagnostics and biosensing. *Wiley Interdiscip Rev Nanomed Nanobiotechnol*, 15 (2023) 1.
- 5 Herizchi R, Abbasi E, Milani M & Akbarzadeh A, Current methods for synthesis of gold nanoparticles. *Artif Cells Nanomed Biotechnol*, 44 (2016) 2.
- 6 Bani-Jaber A, Taha S, Abu-Dahab R, Abdullah S, El-Sabawi D, Al-Masud AA, Aodah AH & Altamimi AA, Preparation and characterization of chitosan–octanoate nanoparticles for efficient delivery of curcumin into prostate cancer cells. *3 Biotech*, 14 (2024) 12.
- 7 Fanelli GN, Dal Pozzo CA, Depetris I, Schirripa M, Brignola S, Bionon P, Balistreri M, Santo LD, Lonardi S, Munari G, Loupakis F & Fassan M, The heterogeneous clinical and pathological landscapes of metastatic BRAF-mutated colorectal cancer. *Cancer Cell Int*, 20 (2020) 1.
- 8 Aboulthana WM, Shousha WG, Essawy EA, Saleh MH & Salama AH, Assessment of the anticancer efficiency of silver *Moringa oleifera* leaves nano-extract against chemically induced colon cancer in rats. *Asian Pac J Cancer Prev*, 22 (2021) 10.
- 9 Jadoun S, Arif R, Jangid NK & Meena RK, Green synthesis of nanoparticles using plant extracts: a review. *Environ Chem Lett*, 19 (2021) 1.
- 10 Okaiyeto K, Hoppe H & Okoh AI, Plant-based synthesis of silver nanoparticles using aqueous leaf extract of *Salvia officinalis*: characterization and antiplasmodial activity. *J Cluster Sci*, 32 (2021) 1.
- 11 Sarwar S, Hossain MJ, Irfan NM, Ahsan T, Arefin MS, Rahman A, Alsubaie A, Alharthi B, Khandaker MU, Bradley DA, Emran TB & azrul Islam SN, Renoprotection of antioxidant-rich foods and probiotics in gentamicin-induced nephrotoxicity in rats. *Life*, 12 (2022) 1.
- 12 Gupta M, Dey S, Marbaniang D, Pal P, Ray S & Mazumder B, Grape seed extract: potential health benefits. *J Food Sci Technol*, 57 (2020) 4.
- 13 Pattanayak M & Nayak PL, Green synthesis of gold nanoparticles using *Elettaria cardamomum* aqueous extract. *World J Nano Sci Technol*, 2 (2013) 1.
- 14 Miliauskas G, Venskutonis PR & Van Beek TA, Screening of radical scavenging activity of medicinal and aromatic plant extracts. *Food Chem*, 85 (2004) 2.
- 15 Re R, Pellegrini N, Proteggente A, Pannala A, Yang M & Rice-Evans C, Antioxidant activity using an improved ABTS radical cation decolorization assay. *Free Radic Biol Med*, 26 (1999) 1231.
- 16 Benzie IF & Strain JJ, Ferric reducing ability of plasma (FRAP) as a measure of antioxidant power. *Anal Biochem*, 239 (1996) 70.
- 17 Oyaizu M, Studies on products of browning reaction: antioxidative activities of products from glucosamine. *Jpn J Nutr Diet*, 44 (1986) 307.
- 18 Woisky RG & Salatino A, Analysis of propolis: parameters and procedures for chemical quality control. *J Apic Res*, 37 (1998) 99.
- 19 Kumari CS, Yasmin N, Hussain MR & Babuselvam M, *In vitro* anti-inflammatory and anti-arthritis properties of *Rhizophora mucronata* leaves. *Int J Pharma Sci Res*, 6 (2015) 3.
- 20 Sakat S, Tupe P & Juvekar A, Gastroprotective effect of *Oxalis corniculata* Linn. methanol extract in experimental animals. *Planta Med*, 76 (2010) 548.
- 21 Schwartz-Duval AS, Konopka CJ, Moitra P, Daza EA, Srivastava I, Johnson EV, Kampert TL, Fayn S, Haran A, Dobrucki LW & Pan D, Intratumoral generation of photothermal gold nanoparticles. *Nat Commun*, 11 (2020) 1.
- 22 Cheng J, Wang X, Qiu L, Li Y, Marraiki N, Elgorban AM & Xue L, Green-synthesized zinc oxide nanoparticles regulate apoptotic expression in MG-63 bone cancer cells. *J Photochem Photobiol B*, 213 (2020) 112070.
- 23 Ganeshkumar M, Sastry TP, Kumar MS, Dinesh MG, Kannappan S & Suguna L, Sunlight-mediated synthesis of gold nanoparticles as carrier for 6-mercaptopurine. *Mater Res Bull*, 47 (2012) 9.
- 24 He X & Lu H, Graphene-supported tunable extraordinary transmission. *Nanotechnology*, 25 (2014) 32.
- 25 Rahman TU, Khan H, Liaqat W & Zeb MA, Phytochemical screening and green synthesis of gold nanoparticles using *Ricinus communis* seed extract. *Microsc Res Tech*, 85 (2022) 1.
- 26 Parvathy CR & Praseetha PK, Anti-diabetic potential of antimicrobial carbon quantum dots from *Vitis vinifera* seeds. *Nano Biomed Eng*, 15 (2023) 1.
- 27 Edwin MH, Sundara Raj AS, Mani A, Sillanpää M & Al-Farraj S, Green synthesis of *Vitis vinifera* extract-appended magnesium oxide nanoparticles. *Nanotechnol Rev*, 13 (2024) 1.
- 28 Ghoreishi SM & Mortazavi-Derazkola S, Eco-friendly synthesis of gold nanoparticles using tangerine peel extract. *Heliyon*, 11 (2025) 1.
- 29 Mariyuchuk R, Smolková R, Bartošová V, Eliašová A, Grishchenko LM, Diyuk VE & Lisnyak VV, The regularities of the *Mentha piperita* L. extract mediated synthesis of gold nanoparticles with a response in the infrared range. *Appl Nanosci*, 12 (2022) 1071.
- 30 Patil N, Shinde D & Patil P, Green synthesis of gold nanoparticles using medicinal plant extracts. *J Appl Organomet Chem*, 3 (2023) 1.
- 31 Kowsalya B & Narendhirakannan RT, Pharmacological potential of *Vitis vinifera*: a comprehensive review. *Suranaree J Sci Technol*, 31 (2024) 6.
- 32 Yilmaz MA, Cakir O, Izol E, Tarhan A, Behcet L & Zengin G, Detailed Phytochemical Evaluation of a Locally Endemic Species (*Campanula baskilensis*) by LC-MS/MS and Its In-Depth Antioxidant and Enzyme Inhibitory Activities. *Chem Biodiversity*, 20 (2023) e202301182.
- 33 Gulcin I, Antioxidants and antioxidant methods: an updated overview. *Arch Toxicol*, 94 (2020) 651.
- 34 Vijayan R, Joseph S & Mathew B, Anticancer and antioxidant activities of green-synthesized silver and gold nanoparticles. *Bioprocess Biosyst Eng*, 42 (2019) 2.
- 35 Shabestarian H, Homayouni-Tabrizi M, Soltani M, Namvar F, Azizi S & Mohamad R, Green synthesis of gold nanoparticles using sumac extract. *Mater Res*, 20 (2016) 1.
- 36 Senthilkumar P, Surendran L, Sudhagar B & Kumar DSRS, Green synthesis of gold nanoparticles from marine algae *Gelidium acerosa*. *SN Appl Sci*, 1 (2019) 1.
- 37 Zayadi RA & Bakar FA, Stability and antioxidant activity of bio-stabilized gold nanoparticles. *J Environ Chem Eng*, 8 (2020) 4.

- 38 Andrés CM, Pérez de la Lastra JM, Juan CA, Plou FJ & Pérez-Lebeña E, Hydrogen peroxide metabolism in mammalian cells. *Stresses*, 2 (2022) 3.
- 39 Uzma M, Prasad D, Sunayana N, Vinay R & Shilpashree H, *In vitro* antioxidant and anti-inflammatory activities of biosynthesized gold nanoparticles. *Mater Technol*, 37 (2022) 1.
- 40 Anitha R, Flumel MJ, Jayakumar K & Gajalakshmi B, Targeted apoptosis in Huh-7 liver cancer cells using *Mentha officinalis*-mediated gold nanoparticles. *J Nanomed Nanotechnol*, 14 (2023) 1.
- 41 Yang X, Bao Y, Zhou X, Zhu H & Gao J, Green synthesis of gold nanoparticles and anticancer activity against cervical cancer. *Arab J Chem*, 17 (2024) 12.
- 42 Darwiche L, Mesmar J, Baydoun E & El Kayal W, Biological and anticancer activities of *Vitis vinifera* varieties. *Int J Mol Sci*, 24 (2023) 17.
- 43 Nirmala JG, Akila S, Nadar MM, Narendhirakannan RT & Chatterjee S, *Vitis vinifera* seed gold nanoparticles induce apoptosis in A431 cells. *RSC Adv*, 6 (2016) 1.
- 44 Grace Nirmala J, Evangeline Celsia S, Swaminathan A, Narendhirakannan RT & Chatterjee S, Cytotoxicity and apoptotic cell death induced by *Vitis vinifera* extracts. *Cytotechnology*, 70 (2018) 1.
- 45 Ali Z, Jabir M & Al-Shammari A, Gold nanoparticles inhibit proliferation of human breast cancer cells. *Res J Biotechnol*, 14 (2019) 79.